

# Flexural Behaviour of Continuous GFRP Reinforced Concrete Beams

By
M. N. Habeeb[*] and A F Ashour[+]

## Abstract

The results of testing two simply and three continuously supported concrete beams reinforced with glass fibre reinforced polymer (GFRP) bars are presented. The amount of GFRP reinforcement was the main parameter investigated. Over and under GFRP reinforcements were applied for the simply supported concrete beams. Three different GFRP reinforcement combinations of over and under reinforcement ratios were used for the top and bottom layers of the continuous concrete beams tested. A concrete continuous beam reinforced with steel bars was also tested for comparison purposes. The experimental results revealed that over-reinforcing the bottom layer of either the simply or continuously supported GFRP beams is a key factor in controlling the width and propagation of cracks, enhancing the load capacity and reducing the deflection of such beams. Comparisons between experimental results and those obtained from simplified methods proposed by ACI 440 committee show that ACI 440.1R-06 equations can reasonably predict the load capacity and deflection of the simply and continuously supported GFRP reinforced concrete beams tested.

---

[*] PhD candidate, EDT4, School of Engineering, Design and Technology, University of Bradford, Bradford BD7 1DP, West Yorkshire, UK.

[+] Senior Lecturer, EDT1, School of Engineering, Design and Technology, University of Bradford, Bradford BD7 1DP, West Yorkshire, UK.

**CE DATABASE SUBJECT HEADINGS:** Concrete; Continuous beams; Fibre composites; Deflection; Flexure, Failure loads; Failure modes; Cracking.

## NOMENCLATURE

$A_f$ Area of GFRP reinforcement

$A_s$ Area of steel reinforcement

$B$ Width of cross-section

$\beta_1$ A strength reduction factor taken as 0.85 for concrete strength up to and including 27.6 MPa. For strength above 27.6 MPa, this factor is reduced continuously at a rate of 0.05 per each 6.9 MPa of strength in excess of 27.6 MPa, but is not taken less than 0.65

$\beta_d$ Reduction coefficient used in calculating deflection

$c_b$ Neutral axis depth for balanced failure

$d$ Beam effective depth

$E_c$ Modulus of elasticity of concrete

$E_f$ Modulus of elasticity of GFRP reinforcement

$E_s$ Modulus of elasticity of steel reinforcement

$f_c'$ Cylinder compressive strength of concrete

$f_{cu}$ Cube compressive strength of concrete

$f_f$ FRP stress at which the concrete crushing failure mode occurs

$f_{fu}$ Ultimate tensile strength of GFRP bars

$\gamma_G$ Proposed reduction factor of 60%, used in calculating deflection of the continuously supported GFRP reinforced concrete beams

| | |
|---|---|
| $I_{cr}$ | Moment of inertia of transformed cracked concrete section |
| $I_g$ | Gross moment of inertia of beam section |
| $I_{\mathrm{e}}$ | Effective moment of inertia of beam section |
| $k$ | Ratio of the neutral axis depth to reinforcement depth |
| $L$ | Beam span |
| $M_a$ | Applied moment |
| $M_{\mathrm{cr}}$ | Cracking moment |
| $n_f$ | Modular ratio between FRP reinforcement and concrete |
| $P$ | Applied load |
| $\varepsilon_{cu}$ | Ultimate strain of concrete |
| $\varepsilon_{fu}$ | Ultimate strain of GFRP reinforcement |
| $\rho_f$ | FRP reinforcement ratio |
| $\rho_{fb}$ | Balanced FRP reinforcement ratio |

## Introduction

Fibre reinforced polymer (FRP) bars are considered as a potential replacement for traditional steel reinforcement in many concrete applications, especially those in severe environment. Such applications necessitate the need for either developing a new design code or adopting and modifying the current ones to account for the engineering characteristics of FRP materials. Consequently, several studies investigated the flexural behaviour of simply supported concrete beams reinforced with different types of FRP reinforcing bars (Almusallam 1997; Al-Sayed et al. 2000; Al-Sayed 1998; Benmokrane et al. 1995, 1996; Grace et al. 1998; Pecce et al. 2000; Rasheed et al. 2004; Theriault and Benmokrane 1998; Toutanji and Deng 2003; Vijay and GangaRao 2001; Toutanji and Saafi 2000; Yost and Gross 2002). A few other studies attempted to develop design equations for predicting deflections of FRP reinforced concrete beams (Abdalla 2002; Aiello and Ombres 2000; Al-Sayed 1993; Arockiasamy et al. 2000; Yost and Gross 2002). ACI 440 committee (2006) introduced a model established through experimental and analytical principles that could predict the flexural moment capacity as well as deflections of concrete members reinforced with FRP bars. The ACI 440.1R-06 equations are a very important step toward the implementation of FRP composites in concrete structures; however the guidelines could be verified and possibly revised when more data become available (Vijay and GangaRao 2001). In a comprehensive study, Vijay and GangaRao (2001) presented a simple mathematical model quoting the ACI 318-99 and ACI-440.1R-01 equations to identify failure modes and to compute moment capacity of 77 simply supported GFRP reinforced concrete beams, extracted from 14 different experimental investigations. They showed that the moment capacity of GFRP reinforced concrete beams could be

accurately predicted. On the other hand, Toutanji and Deng (2003) confirmed on the ability of the ACI-440.1R-01 equations in predicting deflections of GFRP simply supported concrete beams. Generally, the work presented in the literature recognised the potential of the ACI-440.1R-01 equations to predict the moment capacity in addition to deflections of simply supported FRP reinforced concrete beams, particularly GFRP reinforced concrete beams due to the availability of the data on such beams.

Grace et al. (1998) presented test results of continuously supported T-section concrete beams reinforced with different combinations of longitudinal reinforcing bars and stirrups made of GFRP, CFRP and steel bars. The research concluded that while different FRP reinforcement arrangements were found to have the same load capacity as conventional steel reinforced concrete beams, failure modes and ductility differed. It was also observed that the crack pattern is dependent mainly on the type of stirrups used.

This paper investigates the application of GFRP bars as longitudinal reinforcement for continuous concrete beams. Test results of such beams have been compared against those of simply supported beams reinforced with identical GFRP bars and a continuously supported steel reinforced concrete beam. This comparison has been based on failure modes, crack patterns, reinforcement strains, load capacity, load redistribution and deflection of all six beams tested. The present study has evaluated the ACI 440.1R-06 equations for moment capacity and deflection against the experimental results of continuously and simply supported GFRP reinforced concrete beams.

## Test Specimens and Materials

Two simply and three continuously supported GFRP reinforced concrete beams were tested in flexure. In addition, a continuously supported steel reinforced concrete beam was tested for comparison purposes. All beams were 200 mm in width and 300 mm in depth. The continuously supported beams had two spans, each of 2750 mm, whereas the simply supported beams had a span of 2750 mm, as shown in Figures 1 and 2, respectively.

The simply supported beams were designed to achieve two different modes of failure, namely GFRP bar rupture and concrete crushing. The former was accomplished by using reinforcement ratio less than the balanced reinforcement ratio $\rho_{fb}$ as defined in the ACI 440.1R-06 guidelines, and the latter by using reinforcement ratio greater than $\rho_{fb}$ as given in Table 1.

The GFRP reinforced concrete continuous beams were reinforced with three different reinforcement combinations at the top and bottom layers. Beam GcOU was reinforced with six GFRP bars of 15.9mm diameter (over reinforcement) at the top side and three GFRP bars of 12.7mm diameter (under reinforcement) at the bottom side, whereas beam GcUO was reinforced with an opposite arrangement of GFRP longitudinal bars as given in Table 1 and Figure 1. The top GFRP reinforcement of beam GcOO was the same as the bottom reinforcement, each consisting of six 15.9mm diameter GFRP bars (over reinforcement). The longitudinal top and bottom steel reinforcement of the continuously supported control beam ScUU, consisting of four 12 mm diameter steel bars, was selected to have the same tensile strength as the three GFRP bars of 12.7mm diameter used in beams GcUO, GcOU and GsU. Vertical steel stirrups of 8 mm bar

diameter, spaced at 140 mm centres were provided throughout each beam length in accordance with ACI 318-05.

Tensile tests of reinforcing steel and GFRP bar specimens were conducted until rupture. Table 2 details the properties of the entire bar reinforcements used in the beams tested.

Sand, gravel coarse aggregate (10mm maximum size) and ordinary Portland cement were used to produce concrete with a target compressive strength of 40 N/mm$^2$ at 28 days. In total, eighteen 100mm cubes and eighteen 150mm diameter x 300mm high cylinders were made for all beams tested. All test specimens were de-moulded after 24hrs, wet cured and covered with polyethylene sheets until the date of testing. Three cubes and three cylinders were tested immediately after testing of each beam to provide values for cube compressive strength, $f_{cu}$, and cylinder compressive strength, $f_c^{'}$ as presented in Table 1.

## Beam Notations

The notation of each beam is based on the type of reinforcement, nature of support, identification of reinforcement ratio used and location of each reinforcement ratio, either in the top or bottom layer, in case of continuous beams. The first letter in the notation represents the type of reinforcement, 'G' for GFRP and 'S' for steel reinforcement. The second letter corresponds to the supporting system, either 'c' for continuously supported beams or 's' for simply supported beams. The third letter, which could be 'U' for under reinforcement ratio or 'O' for over reinforcement ratio, illustrates the bottom reinforcement ratio for the simply supported beams, meanwhile

represents the top reinforcement ratio for the continuously supported beams. The fourth letter, which is used only for the continuously supported beams, demonstrates its bottom reinforcement ratio, 'U' or 'O'. As an illustrative example, the beam notation GcOU indicates a GFRP reinforced continuously supported beam, with an over and under reinforcement ratios of GFRP bars located at the top and bottom layers of the beam, respectively.

## Test Procedure

Each continuous test beam comprised of two equal spans supported on two roller supports, one at the end and the other at the middle, in addition to a hinge support at the other end of the beam, as shown in Figure 1. Each span of continuous beams was loaded at its mid point via a hydraulic ram and an independent steel reaction frame bolted to the laboratory floor. The simply supported beams were similarly loaded at its mid span and supported on hinge support at one end and a roller support at the other end as depicted in Figure 2. Three load cells were used to measure the reactions at one end support, the middle support in case of continuous beams and at the main applied load from the hydraulic ram as shown in Figure 1. The mid-span deflections were measured by positioning linear variable differential transformers (LVDTs) at the two mid-spans of the continuous beams and the mid-span of the simply supported beams. For quality control purposes, dial gages were also placed adjacent to each LVDT to measure the mid-span beam deflection manually. Additional dial gages were located at the three supports of continuous beams to assess any settlement that might take place during the loading process, which would affect the mid-span deflection readings and the reaction distribution. Load cells and LVDT readings were registered automatically at each load increment at a rate of 6.2kN, using data logging equipment.

Failure of the tested beams was judged to occur when the beam under testing could not uphold any additional applied load. At such stage the applied load was released and no further data were registered by the data logging equipment.

## Test Results and Discussions

### Failure Modes

Four different failure modes were observed throughout the experimental tests as given in Table 3 and explained below.

*Mode 1: Bar rupture*—This mode was illustrated by beams GcOU and GsU. These beams were reinforced with an under-reinforcement ratio of GFRP bars at the bottom layer. Thus, it was expected that the strain in the GFRP reinforcement would reach its ultimate limit, at the mid-span failed section, before the full exhaustion of the ultimate concrete strain, which usually leads to such failure mode, as shown in Figure 3.

*Mode 2: Concrete crushing*—This failure mode was experienced by beams GcUO and GsO, which were reinforced with an over-reinforcement ratio of GFRP bars at the bottom layer. Such reinforcement was the reason behind the concrete crushing at the mid-span section before reaching the ultimate strain value of the GFRP reinforcing bars as revealed in Figure 4. In case of the continuous beam GcUO, wide cracks appeared over the middle support section before concrete crushing at the mid-span section. However, the strain recorded at the top GFRP reinforcement was much less than the GFRP rupture strain, indicating that debonding of top GFRP reinforcement may have occurred as explained later.

*Mode 3: Concrete crushing combined with shear failure*—Beam GcOO exhibited this mode of failure as shown in Figure 5. The diagonal shear cracks, which emerged at a late stage of loading, propagated simultaneously with the flexural concrete crushing mode of failure up to the sudden collapse and the disintegration of the beam. In comparison to beam GcUO, beam GcOO developed a higher compression resistance at the top layer of the failed section due to the presence of a higher amount of GFRP reinforcement. Such enhancement in compression allowed the shear force to participate in the failure process; whereas the top layer of beam GcUO did not resist the compression force to a limit that would allow enough time for the shear force to participate fully in the failure process.

*Mode 4: Conventional ductile flexural failure mode*—This mode was demonstrated by the steel reinforced concrete beam ScUU. It occurred due to yielding of tensile steel reinforcement followed by concrete crushing at both middle support and mid-span sections as shown in Figure 6.

## Crack Propagation and Reinforcement Strains

The first cracking load of each beam tested is presented in Table 3. The table indicated that the steel reinforced concrete beam cracked at a later stage, in comparison to its similar continuously supported GFRP reinforced concrete beam. This could be attributed to the higher modulus of elasticity of steel bars than that of GFRP bars. The table also revealed that the two over-reinforced GFRP beams at the bottom layer, beams GcOO and GcUO, showed the first mid-span crack at a slightly

higher load than that of the mid-span under-reinforced GFRP beam GcOU. It could be also noticed that, for the same two beams GcOO and GcUO, the first crack over the middle support started earlier than that at the mid-span. In contrast, beam GcOU developed an earlier crack at its mid-span than middle support.

In general, cracking in the flexural span of all beams tested consisted predominantly of vertical flexural cracks. The steel beam ScUU demonstrated similar vertical flexural crack pattern as the under-reinforced GFRP continuous beam GcOU. As the load was increased, shear stresses became influential and induced inclined cracks in beams GcOO and GcUO. These cracks diagonally propagated toward the vicinity of load points on the compressive side of these two beams.

Figures 7 and 8 present the crack width at the middle support and mid-span of the beams tested, respectively. Beam ScUU demonstrated the least crack width among all beams tested. It could be also noticed that the GFRP beams reinforced with over reinforcement ratio at their bottom layer, beams GcUO, GcOO and GsO, had considerably less crack width at mid-span sections than the under reinforced GFRP beams, GcOU and GsU, as shown in Figure 8. The simply supported GFRP beams accomplished a similar crack propagation trend as its corresponding continuously supported beams that reinforced with identical bottom reinforcement, as seen in Figure 8.

Figure 9 presents the total applied load against tensile strains in the top reinforcement over the central support and bottom reinforcement at mid-span for the continuously supported beams tested. Tensile strains in GFRP reinforcing bars increased

significantly after concrete cracking. At a given load, strains in GFRP bars were higher than those in steel bars before yielding.

Strains in top GFRP bars over the central support were larger than those in bottom bars at midspan for the three continuous beams GcOU, GcUO and GcOO. Strains in GFRP bars of beam GcOU are larger than those of the other two continuous beams GcUO and GcOO. Although wide cracks over the central support of beams GcUO and GcOO were observed before failure, recorded strains in top GFRP bars of these two beams were much less than the rupture strains as shown in Figure 9, indicating local debonding between top GFRP bars and concrete.

## Load Capacity

Failure loads of the beams tested are plotted in Figure 10 and presented in Table 3. Over-reinforced simply supported beam GsO failed at nearly 50% of the total failure load of beams GcUO and GcOO. Similarly beam GsU failed at nearly 40% of the total failure load of beam GcOU. Such harmony in comparison between the load capacity of the simply and continuously supported GFRP reinforced concrete beams is attributed to the identical reinforcement ratio at the bottom layer of each compared set of beams. Beams GcUO and GcOO have tolerated more loads than beam GcOU as beam GcOU is reinforced with under-reinforcement ratio of GFRP bars at the bottom layer.

Even though the area of the top GFRP reinforcement used in beam GcOO was three times higher than that used in beam GcUO, beam GcOO resisted a slightly higher

failure load (1.3 %). This indicates that GFRP top reinforcement was ineffective in enhancing the beam load carrying capacity.

In spite of the under-reinforcement ratio used for the top and bottom layers of steel reinforced concrete continuous beam ScUU, this beam accomplished similar load capacity as beam GcOO, which in contrast to beam ScUU, reinforced with over-reinforced ratio of GFRP bars at the top and bottom layers as indicated in Table 3.

## Prediction of Loads and Modes of Failure

The ACI 440.1R-06 report, based on the balanced FRP reinforcement ratio $\rho_{fb}$ obtained from Eq. 1 below, predicted the moment capacity $M$ of beams reinforced with FRP bars using Eqs. 2 and 3 when the reinforcement ratio $\rho_f$ is greater than $\rho_{fb}$, and by applying Eqs. 4 and 5 when the reinforcement ratio $\rho_f$ is less than $\rho_{fb}$.

$$\rho_{fb} = 0.85\beta_1 \frac{f_c^{'}}{f_{fu}} \frac{E_f \varepsilon_{cu}}{E_f \varepsilon_{cu} + f_{fu}} \tag{1}$$

$$M = \rho_f f_f (1 - 0.59 \frac{\rho_f f_f}{f_c^{/}}) bd^2 \tag{2}$$

$$f_f = \sqrt{\frac{(E_f \varepsilon_{cu})^2}{4} + \frac{0.85\beta_1 f_c^{'}}{\rho_f} E_f \varepsilon_{cu}} - 0.5 E_f \varepsilon_{cu} \le f_{fu} \tag{3}$$

$$M = A_f f_{fu} (d - \frac{\beta_1 c_b}{2}) \tag{4}$$

$$c_b = \left( \frac{\varepsilon_{cu}}{\varepsilon_{cu} + \varepsilon_{fu}} \right) d \tag{5}$$

where $\rho_f$ $(= A_f / bd)$ is the FRP reinforcement ratio, $A_f$ is the area of FRP reinforcement, $b$ and $d$ are the width and effective depth of the GFRP reinforced concrete beam, $f_c^{'}$ is the cylinder compressive strength of concrete, $f_{fu}$ is the ultimate tensile strength of FRP bars, $\varepsilon_{cu}$ is the ultimate strain in concrete, $E_f$ is the modulus of elasticity of FRP bars, $f_f$ is the FRP stress at which the concrete crushing failure mode occurs, $c_b$ is the neutral axis depth for balanced failure as defined in Eq. (5) and $\beta_1$ is a strength reduction factor taken as 0.85 for concrete strength up to and including 27.6 MPa. For strength above 27.6 MPa, this factor is reduced continuously at a rate of 0.05 per each 6.9 MPa of strength in excess of 27.6 MPa, but is not taken less than 0.65.

For the simply supported GFRP reinforced concrete beams GsO and GsU, the beam load capacity $P$ is estimated by satisfying the equilibrium condition at the mid-span critical section ($M=Pl/4$, where $M$ is the moment capacity calculated using the ACI 440.1R-06 equations presented above and $l$ is the beam span).

The load capacity of continuously supported GFRP reinforced concrete beams is chosen to be the lower load that causes the accomplishment of the moment capacity of either mid-span or middle support section. This is mainly due to the brittle nature of concrete crushing or FRP rupture mode of failure. The elastic moments at the designated critical sections of a continuously supported beam are $0.156Pl$ and $0.188Pl$ for the mid-span and middle-support sections, respectively, where $P$ and $l$ are the mid span applied load and beam span, respectively. The self weight of beams tested is negligible compared with the failure load; therefore it is not included in the above calculation.

The predicted and experimental failure loads for each beam tested is presented in Table 3 and plotted in Figure 10. The ACI 440.1R-06 equation reasonably predicted the load capacity of the simply supported beam GsU and significantly underestimated the load capacity of beam GsO. This may be attributed to the difficulty in predicting the concrete crushing strain, $\varepsilon_{cu}$, which, in turn, has a major impact on stresses $f_f$ in GFRP bars obtained from Eq. (3) when failure occurs due to concrete crushing. In addition, the ACI 440 equation ignores the reinforcement at the compression zone which would have some additional influence on the underestimation of the predicted moment capacity. The tensile rupture and concrete crushing modes of failure are correctly predicted by the ACI 440.1R-06 method for beams GsU and GsO, respectively.

As for the continuously supported GFRP reinforced concrete beams, the load and location of failure of beam GcOU were reasonably predicted by the ACI 440.1R-06 equations. A continuous beam reinforced similarly to beam GcOU in this study was tested by Grace et al. (1998). The ACI 440.1R-06 equations also reasonably predicted the load capacity for the Grace beam. Such successful predictions strengthen the belief in the credibility of the ACI 440.1R-06 equations in estimating the failure of continuous beams under-reinforced with GFRP bars in the bottom layer.

However, the ACI 440.1R-06 equations predicted that beams GcUO and GcOO would fail at much lower loads than those recorded in experiments as it could be seen from Table 3 and Figure 10. The application of the previously detailed principle, of choosing the lower load that would achieve the moment capacity at either the mid-span or middle support section, predicted the failure location of beams GcOO and

GcUO to take place at the middle support that has not been fulfilled in the actual experimental tests. This is mainly attributed to the wide cracks that were developed over the middle support section of both beams (see Figure 7) due to debonding of top GFRP bars which turned the continuously supported beam into two over reinforced simply supported beams. Thus the failure was eventually occurred at the mid-span sections. To validate this justification, Figure 10 illustrated the ACI 440-1R-06 prediction of the load capacity for one span of beams GcOO and GcUO, as a simply supported beam subjected to a mid-span point load. The comparison between the ACI 440.1R-06 failure load prediction of beams GcOO and GcUO at their simply and continuously supported status authenticated the above assumption. This behaviour explains the strain values of the top reinforcement bars of both beams near failure, which were much less in comparison to their ultimate strain limit, as it could be demonstrated in Figure 9 and Table 2.

The capacity reduction factor recommended by ACI 440-06 was developed based on test data of simply supported beams. As the ACI 440 equations are more conservative in predicting failure loads for the simply supported beams than continuous beams tested, as shown in Figure 10 and Table 3, the use of the same capacity reduction factor recommended by ACI 440-06 when designing continuous beams would be less conservative. Such conclusion should be further investigated when more test results become available.

## Redistribution of Support Reactions

Reactions recorded at middle and end supports for each continuous beam are presented in Figure 11. To asses the load redistribution of each beam the elastic reactions at the middle and end supports, considering a uniform flexure stiffness '*EI'* throughout the entire beam, are also plotted in the same figure. Due to the ductile behaviour of the steel bars, it was expected that beam ScUU would demonstrate distinctive load redistribution in comparison to the GFRP reinforced concrete beams. Such anticipation has not been shown in Figure 11 due to the following reasons:

- The loading system illustrated in Figure 1 produced a small difference between the moment values at mid-span and the middle support.
- The identical reinforcement (4 bars of 12mm. diameter) used at the top and bottom layers of the steel reinforced concrete beam tested caused similarity in strains of the top and bottom bars as illustrated in Figure 9, where the yielding point for the top and bottom steel reinforcement was near enough to be compatible.

Beam GcOO demonstrated similar unremarkable moment redistribution behaviour to beam ScUU. This would be mainly accredited to the brittle nature of the GFRP bars.
Beams GcUO and GcOU behaved slightly dissimilar to beam GcOO, due to the variation of the flexure stiffness '*EI'* throughout the entire length of these two beams, which is attributed to the difference in the amount of reinforcement at the top and bottom layers. Further to that, the reverse reinforcement arrangement used for beam GcOU in comparison to beam GcUO demonstrated the opposite way of reaction response for these two beams.

## Mid-span Deflection

The experimental load against mid-span deflection curves of the steel and GFRP reinforced concrete beams tested are presented in Figure 12. Each curve represents the average of two readings of deflection obtained from LVDTs and dial gauges at the mid-span of each beam tested. For continuous beams, recorded mid-span deflections at one side were similar to those at the other side, therefore one side mid-span deflections are presented in Figure 12.

Initially, all tested beams were un-cracked where they exhibited linear load-deflection behaviour. This is accredited to the linear elastic characteristics of concrete, GFRP bars, as well as steel bars before reaching the yielding point. With the increment of additional loading, cracking occurred at the mid-span of each beam, causing a reduction in stiffness. As the GFRP reinforced concrete beams demonstrated wider crack openings than the steel reinforced concrete beam, they exhibited higher mid-span deflections, as it could be seen from Figure 12.

Beam GcOU exhibited the highest deflection among the GFRP continuous beams, due to the low stiffness of its bottom reinforcement ($E_f A_f$ =16808 kN) in comparison to that of the other two continuous GFRP reinforced concrete beams GcOO and GcUO ($E_f A_f$ =46057 kN). The over-reinforcement ratio used at the top layer of beam GcOO, which was equivalent to more than 3.3 times of the reinforcement ratio used for the same layer in beam GcUO, had a marginal effect on the reduction of the deflection of this beam in comparison to that of beam GcUO as shown in Figure 12. Beam GsO deflected less than beam GsU as the bottom GFRP reinforcement used in beam GsO had higher stiffness, $E_f A_f$, than that of the bottom GFRP bars in beam GsU.

## Deflection Prediction

The immediate deflection of simply and continuously supported reinforced steel concrete beams loaded with a mid-span point load illustrated in Figures 1 and 2, could be calculated by Eqs. (6) and (7), respectively, as given below:

$$\Delta = \frac{Pl^3}{48E_c I_e} \tag{6}$$

$$\Delta = \frac{7}{768}\frac{Pl^3}{E_c I_e} \tag{7}$$

where $P$ is the mid-span applied load at which the deflection is computed, $l$ is the span length, $E_c$ is the modulus of elasticity of concrete and $I_e$ is the effective moment of inertia of the beam section. A modified expression for the effective moment of inertia $I_e$ to be used for predicting the deflection of FRP reinforced concrete beams is given by ACI 440 committee as follows:

$$I_e = \left[\frac{M_{cr}}{M_a}\right]^3 \beta_d I_g + \left[1 - \left[\frac{M_{cr}}{M_a}\right]^3\right] I_{cr} \le I_g \tag{8}$$

where $M_{cr}$ is the cracking moment = $2\, f_{cr}\, I_g / h$, $M_a$ is the applied moment, $\beta_d$ is a reduction coefficient = $[(0.2\rho_f/\rho_{fb}) \le 1]$, $I_g$ is the gross moment of inertia = $bh^3/12$, $h$ is the overall height of the concrete beam, $I_{cr}$ is the moment of inertia of transformed cracked section = $\left(bd^3/3\right)k^3 + n_f A_f d^2 (1-k)^2$, $k$ is the ratio of the neutral axis depth to reinforcement depth = $\sqrt{(\rho_f n_f)^2 + 2\rho_f n_f} - \rho_f n_f$, $n_f$ = $(E_f/E_c)$ is the modular

ratio between the FRP reinforcement and concrete, $E_c = 4750\sqrt{f_c'}$ (N/mm$^2$) and $f_{cr}$ is the modulus of rupture of concrete $= 0.62\sqrt{f_c'}$ (N/mm$^2$).

Comparisons between experimental load-deflection curves obtained in this study and those predicted by the ACI 440.1R-06 equations at mid-span of the simply supported beams are presented in Figure 13. The curves show that there is a good agreement between the experimental and predicted deflection values for the simply supported GFRP reinforced concrete beams tested.

For continuous members, the ACI 318-05 stated that the use of the mid-span section properties is considered satisfactory in approximate deflection calculation primarily because the mid-span rigidity (including the effect of cracking) has the dominant effect on deflection. Furthermore, the ACI 318-05 also suggests, alternatively, using the average $I_e$ at the critical positive and negative moment sections for deflection calculation. The ACI 318-95 (Portland Cement Association 1996) recommends that the above mentioned average of $I_e$ could be obtained, for beams with one continuous end, by the following formula:

$$I_e = 0.85I_m + 0.15I_{cont.end} \quad (9)$$

where $I_m$ refers to $I_e$ at the mid-span section and $I_{cont.end}$ refers to $I_e$ at the middle support section. The above mentioned two methods were implemented to predict the deflection of the GFRP continuous beams tested. Comparisons between experimental load-deflection curves obtained in this study and those predicted by the above mentioned suggestions for the continuously supported GFRP tested beams are

presented in Figures 14 (for Beam GcOU), 15 (for Beam GcUO) and 16 (for Beam GcOO).

Figure 14 illustrates that the experimental deflection of beam GcOU compared well with the predicted deflection, by applying Eq. 8 for the mid-span section only. Meanwhile, using the same method for beams GcUO and GcOO, shows a reasonable comparison to the experimental results, with a steady under estimation of the deflection up to nearly 50% of the failure load. As the load was increased, this underestimation has progressively increased till the end of loading due to the sudden increase of the over support crack width, as shown in Figure 7, which took place almost at the same percentage of 50 % of the failure load, as given in Figures 15 and 16. To overcome the shortcomings of the previous methods, a reduction factor, $\gamma_G$, has been applied to the second term of the ACI 440-06 equation (Eq. (8)), which represents the post cracking phase, as below:

$$I_e = \left[\frac{M_{cr}}{M_a}\right]^3 \beta_d I_g + \left[1 - \left[\frac{M_{cr}}{M_a}\right]^3\right] I_{cr} \gamma_G \qquad (10)$$

A reduction factor, $\gamma_G$, of 60% was found to be an effective tuning parameter for the deflection prediction as it could be seen in Figures 14, 15 and 16. Further test results would be required to authenticate the proposed value of $\gamma_G$.

## Conclusions

Based on the work described in this paper, the following conclusions are drawn:

- Due to the lower elastic modulus of GFRP bars, continuously supported GFRP reinforced concrete beams can develop earlier and wider cracks than similar steel reinforced concrete beams.
- The proposition of the ACI 318-05, regarding the spacing of steel stirrups, has to be reconsidered to avoid shear failure when GFRP bars are used as longitudinal reinforcement for continuously supported concrete beams with steel stirrups.
- Continuously supported GFRP reinforced concrete beams do not demonstrate any remarkable load redistribution.
- Over reinforcing the bottom layer of simply and continuously supported concrete beams by GFRP bars could be a key factor in enhancing the load capacity, controlling the deflection, in addition to the delay of crack propagation at the mid-span section of such beams.
- Increasing the top layer reinforcement of continuously supported GFRP reinforced concrete beams does not contribute significantly in improving the load capacity and deflection reduction.
- Load capacity and deflection of GFRP simply supported concrete beams could be reasonably predicted using ACI 440.1R-06 equations.
- The ACI 440.1R-06 equations seem to be effective in predicting the load capacity and deflection of the under-reinforced at the bottom layer GFRP continuously supported concrete beams. As for the over-reinforced at the bottom layer GFRP continuously supported beams, the prediction process has been negatively affected by the wide cracks appeared over the intermediate support, which eventually turned the continuous beams into two simply supported beams.

- The ACI 440.1R-06 equations could reasonably predict the deflection of GFRP continuous beams with a slight steady under-estimation before the occurrence of wide cracks over the middle support. A proposed reduction factor of 60% for the post cracking term for estimating the effective moment of inertia proposed by ACI 440-06, has been found to be effective in tuning the deflection prediction of continuously supported GFRP reinforced concrete beams.

## *References*


1. Abdalla, H. (2002). "Evaluation of Deflection in Concrete Members Reinforced with Fibre Reinforced Polymer (FRP) Bars," Journal of Composite Structures, 56 (1), 63-71.
2. ACI committee 440 (2006). **"**Guide for the Design and Construction of Structural Concrete Reinforced with FRP bars", 44 pages.
3. ACI Committee 318 (2005). "Building Code Requirements for Structural Concrete (ACI 318-05) and Commentary (ACI 318R-05)", 318R-152, 318R-103.
4. Aiello, A. and Ombres, L. (2000). "Load-Deflection Analysis of FRP Reinforced Concrete Flexural Members," Journal of Composites for Construction, 4 (4), 164-171.
5. Almusallam, T. H. (1997). "Analytical prediction of flexure behavior of concrete beams reinforced with FRP bars" Journal of Composites Material, 31 (7), 640-57.
6. Al-Sayed, S. H., AL-Salloum , Y. A., and Almusallam, T. H.(2000). "Performance of Glass Fibre reinforced Plastic Bars as a Reinforcing Material for Concrete Structures," Composites: Part B, 31(6-7), 555-567.
7. Al-Sayed, S.H. (1998). "Flexure Behaviour of Concrete Beams Reinforced with GFRP Bars," Cement and Concrete Composites, 20 (1), 1-11.
8. Al-Sayed, S., H. (1993). "Flexural Deflection of Reinforced Fibrous Concrete Beams," ACI Structural Journal, 90 (1), 72-75.
9. Arockiasamy, M., Chidambaram, S., Amer, A., and Shahawy, M. (2000). "Time-Dependent Deformations of Concrete Beams Reinforced with CFRP Bars," Composites Engineering, Part B, 31(6-7), 577-592.

10. Benmokrane, B., Chaallal, O., and Masmoudi, R. (1995).“Glass fiber reinforced plastic (GFRP) rebars for concrete structures,” Construction and Building Materials, 9 (6), 353-364.
11. Benmokrane, B., Chaallal, O., and Masmoudi, R. (1996).“Flexural Response of Concrete Beams Reinforced with FRP Reinforcing Bars,” ACI Structural Journal, 93 (1), 46-53.
12. Grace, N. F., Soliman, A. K., Abdel-Sayed, G., and Saleh K. R. (1998). “Behavior and Ductility of Simple and Continuous FRP Reinforced Beams” Journal of Composites for Construction, 4 (2), 186-194.
13. Pecce, M., Manfredi, G., and Cosenza, E.(2000).“Experimental Response and Code Models of GFRP RC Beams in Bending,” Journal of Composites for Construction, 4 (4), 182-187.
14. Portland Cement Association (1996). “Notes on ACI 318-95 Building Code Requirements for Structural Concrete”, Skokie, Illinois.
15. Rasheed, H. A., Naye, I. R., and Melhem, H. (2004). “Response prediction of concrete beams reinforced with FRP bars” Composites Structures, 65 (2), 193-204.
16. Theriault, M. and Benmokrane, B. (1998). “Effects of FRP Reinforcement Ratio and Concrete Strength on Flexure Behaviour of Concrete Beams,” Journal of Composites for Construction , 2 (1), 7-16.
17. Toutanji, H. and Deng, Y. (2003). “Deflection and crack-width Prediction of Concrete Beams Reinforced with Glass FRP Rods,” Construction and Building Materials, 17 (1), 69-74.

18. Vijay, P. V. and GangaRao, H. V. V.(2001). “Bending Behavior and Deformability of Glass Fibre-Reinforced Polymer Reinforced Concrete Members,” ACI Structural Journal, 98(6), 834-842.
19. Toutanji, H. and Saafi, M.(2000). “Flexure Behavior of Concrete Beams Reinforced with Glass Fiber-Reinforced Polymer (GFRP) Bars,” ACI Structural Journal, Technical Paper, 97 (5), 712-719.
20. Yost, J. R. and Gross, S. P. (2002). “Flexure Design Methodology for Concrete Beams Reinforced with Fibre-Reinforced Polymers,” ACI Structural Journal, 99 (3), 308-316.

## List of Tables

## List of Figures

Table1: Details of test specimens

| Beam Notation | Length (mm.) | Top Reinforcement Details | | | | Bottom Reinforcement Details | | | | Concrete Compressive Strength ($N/mm^2$) | |
|---|---|---|---|---|---|---|---|---|---|---|---|
| | | No. | Bar Diameter (□mm) | Reinforcement % | | No. | Bar Diameter (□mm) | Reinforcement % | | $f_c'$ | $f_{cu}$ |
| | | | | $\rho_f$% | $\rho_{fb}$% | | | $\rho_f$% | $\rho_{fb}$% | | |
| GcOU | 5500 | 6 | 15.9 | 2.2 | 0.5 | 3 | 12.7 | 0.6 | 0.7 | 29 | 36 |
| GcUO | 5500 | 3 | 12.7 | 0.6 | 0.7 | 6 | 15.9 | 2.3 | 0.5 | 29 | 35 |
| GcOO | 5500 | 6 | 15.9 | 2.1 | 0.5 | 6 | 15.9 | 2.1 | 0.5 | 25 | 31 |
| GsO | 2750 | 2 | 15.9 | 0.7 | 0.5 | 6 | 15.9 | 2.2 | 0.5 | 26 | 33 |
| GsU | 2750 | 2 | 12.7 | 0.4 | 0.8 | 3 | 12.7 | 0.7 | 0.8 | 29 | 36 |
| ScUU | 5500 | 4 | 12.0 | 0.8 | 3.7 | 4 | 12.0 | 0.8 | 3.7 | 26 | 32 |

- All beams tested had identical cross section of 200mm width and 300mm height.

Table 2: Properties of reinforcement used in beams tested

| Type of Bars | Bar Diameter (mm.) | Young's Modulus, $E$ ($kN/mm^2$) | Ultimate Strength $f_u$ ($N/mm^2$) | Yield Strength $f_y$ ($N/mm^2$) | Ultimate Strain |
|---|---|---|---|---|---|
| Steel (Stirrups) | 8.0 | 206.8 | 611.6 | 525.5 | N/A |
| Steel (longitudinal bars) | 12.0 | 200.0 | 594.4 | 510.8 | N/A |
| GFRP | 12.7 | 44.2 | 605.0 | N/A | 0.015 |
| GFRP | 15.9 | 38.7 | 703.0 | N/A | 0.018 |

Table 3: First visible cracking loads, and failure modes and loads of beams tested

| Beam Notation | First visible cracking load, P (kN) | | Total failure load, 2P (kN) | | | Experimental modes of failure |
|---|---|---|---|---|---|---|
| | | | Experimental | ACI prediction* | | |
| | Mid-span | Middle support | | Mid-span | Middle support | |
| GcOU | 17.7 | 14.6 | 290.2 | 287.7 | 321.4 | Mid-span FRP rupture |
| GcUO | 8.3 | 17.7 | 328.7 | 357.7 | 229.0 | Mid-span concrete crushing |
| GcOO | 8.0 | 24.0 | 333.0 | 336.2 | 279.0 | Mid-span concrete crushing combined with shear failure |
| GsO | 16.6 | N/A | 163.0 | 112.5 | N/A | Concrete crushing |
| GsU | 9.2 | N/A | 118.8 | 92.3 | N/A | GFRP rupture |
| ScUU | 46.9 | 46.9 | 332.3 | 350.9 | | Flexure/Tension |
| * ACI 440-06 and ACI 318-05 were used for GFRP and steel beams, respectively. | | | | | | |

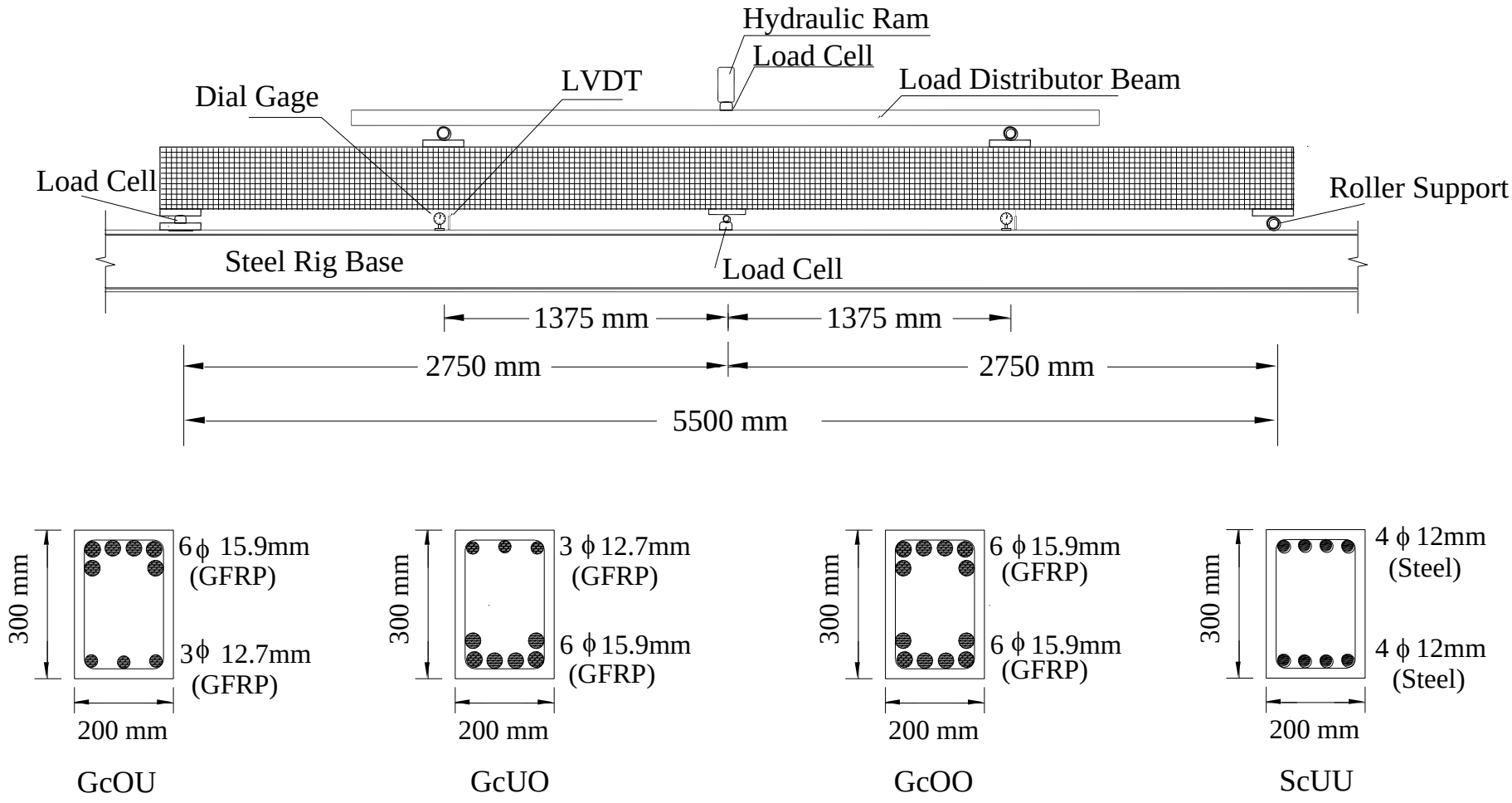


Figure 1: Experimental loading system and cross-section details of continuous beams

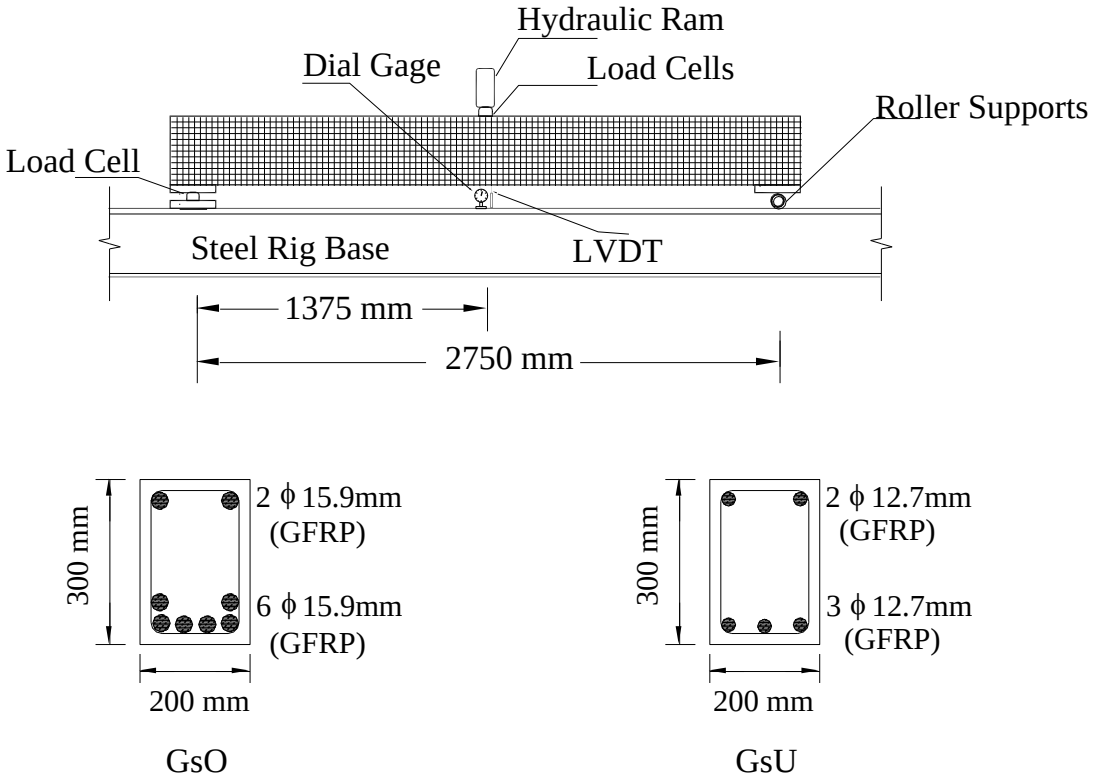


Figure 2: Experimental loading system and cross-section details of simply supported beams

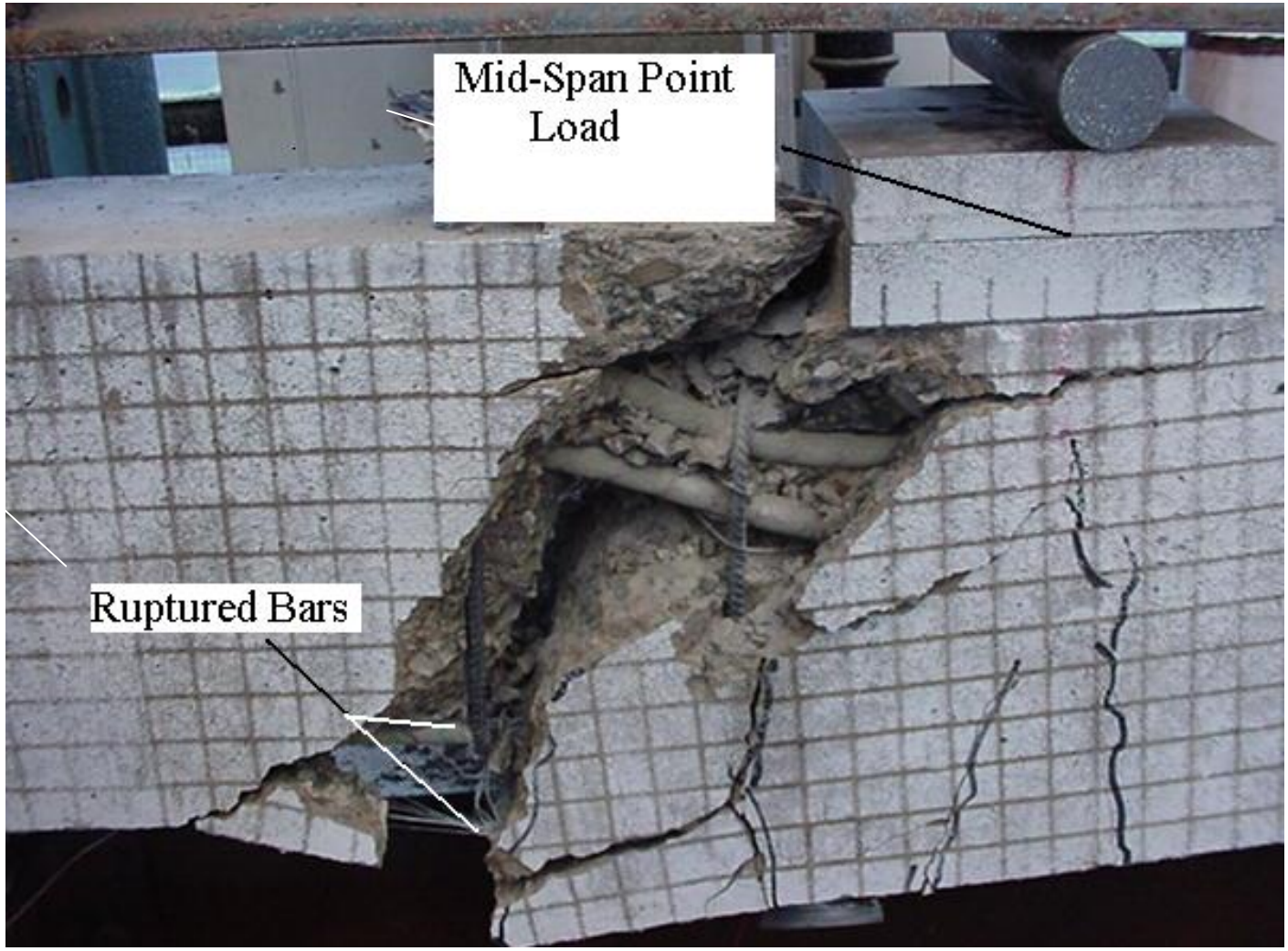


Figure 3: GFRP bar rupture at bottom layer of beam GcOU

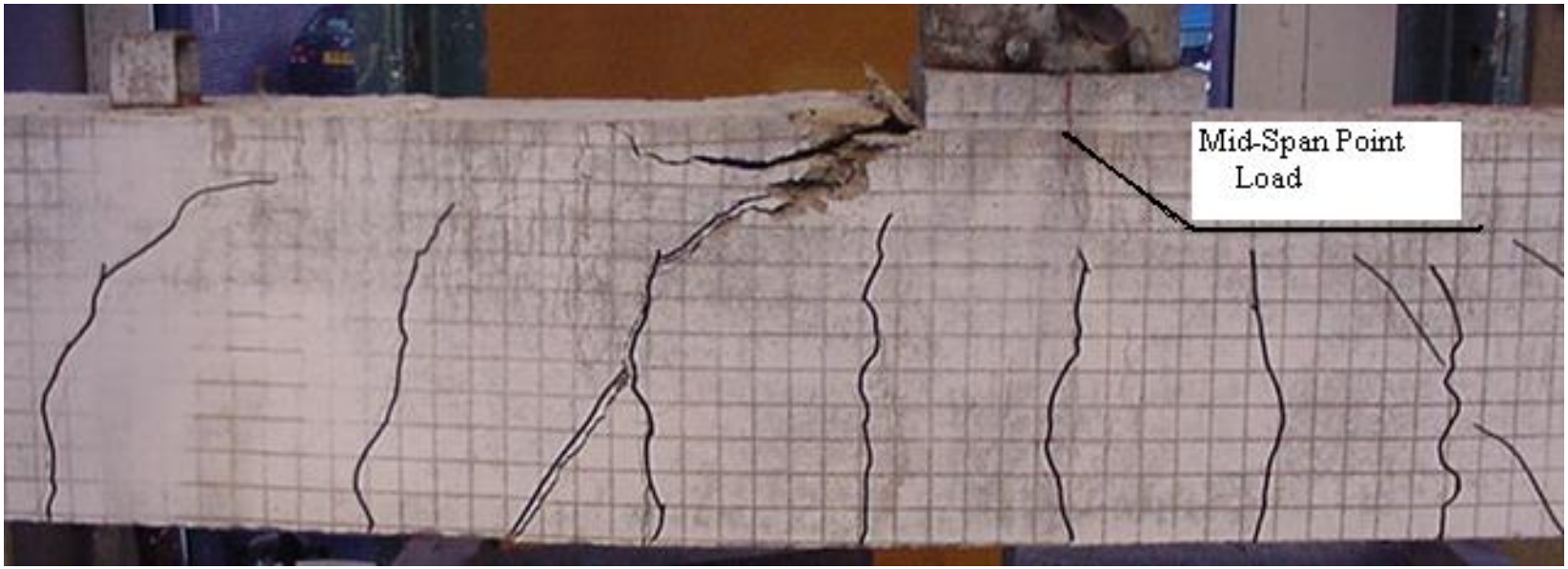


Figure 4: Concrete crushing failure mode of beam GsO


Figure 5: Flexure-shear failure of beam GcOO

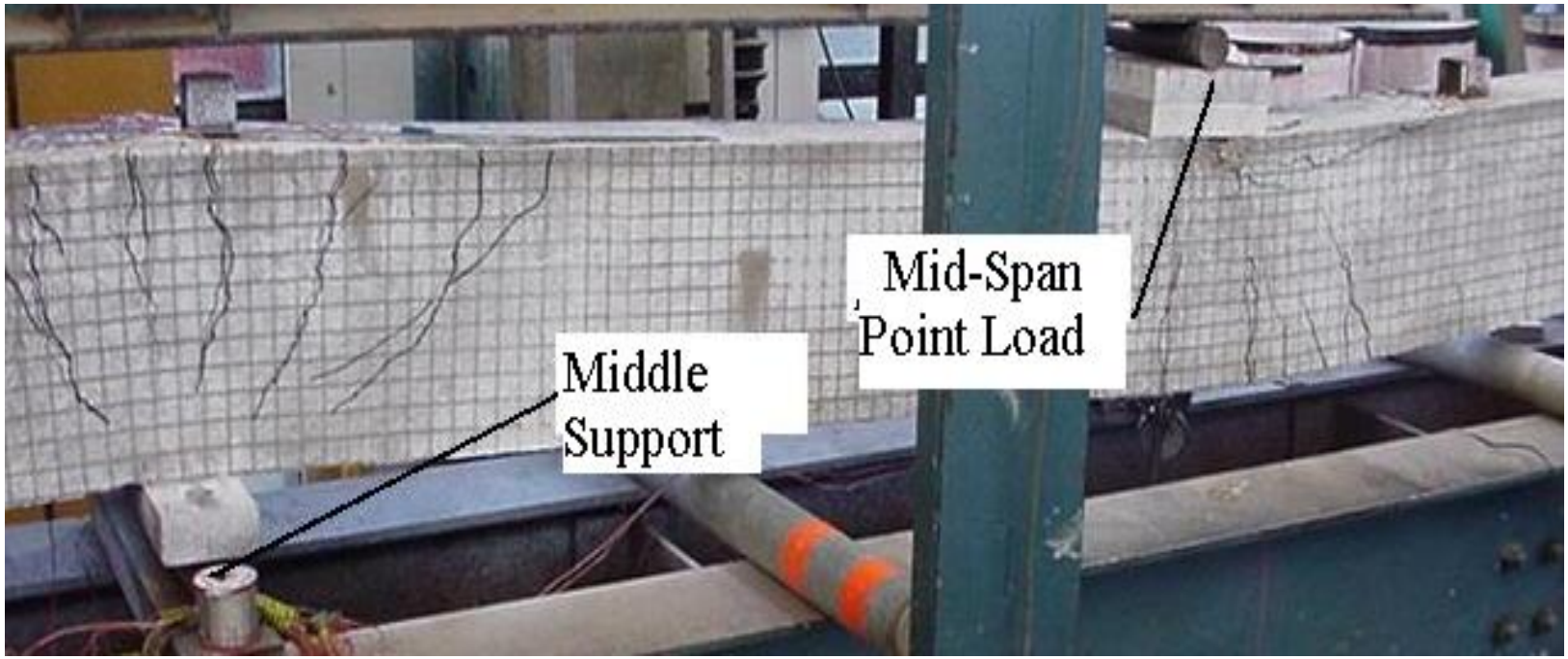


Figure 6: Flexure-tension failure mode of beam ScUU

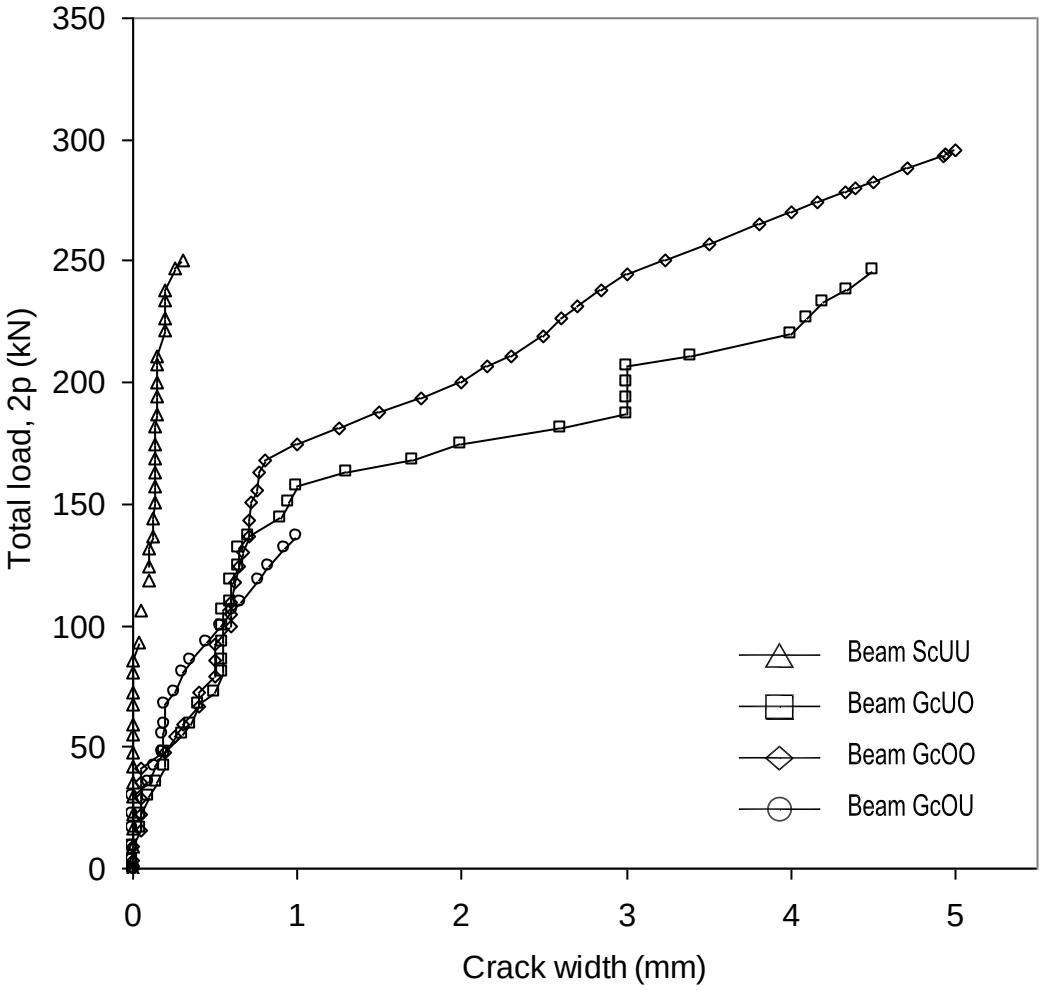


Figure 7: Middle support crack width of continuously supported beams tested

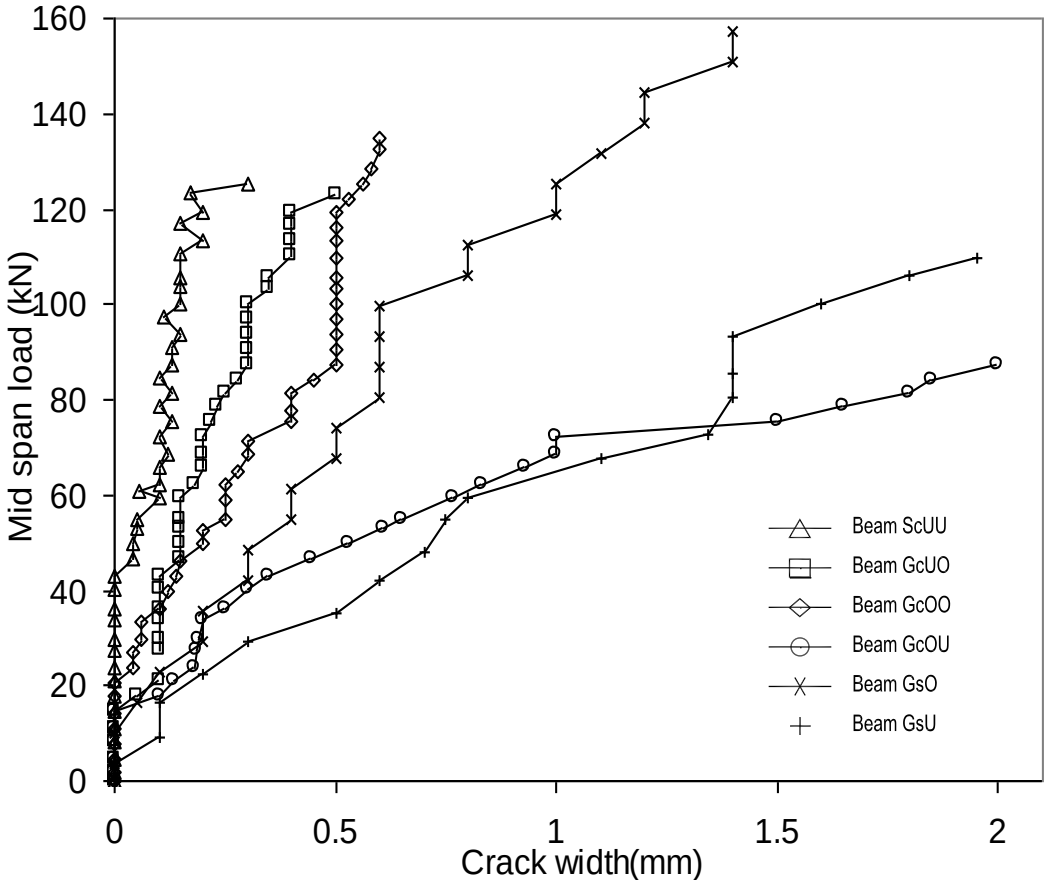


Figure 8: Mid-span crack width of the tested beams

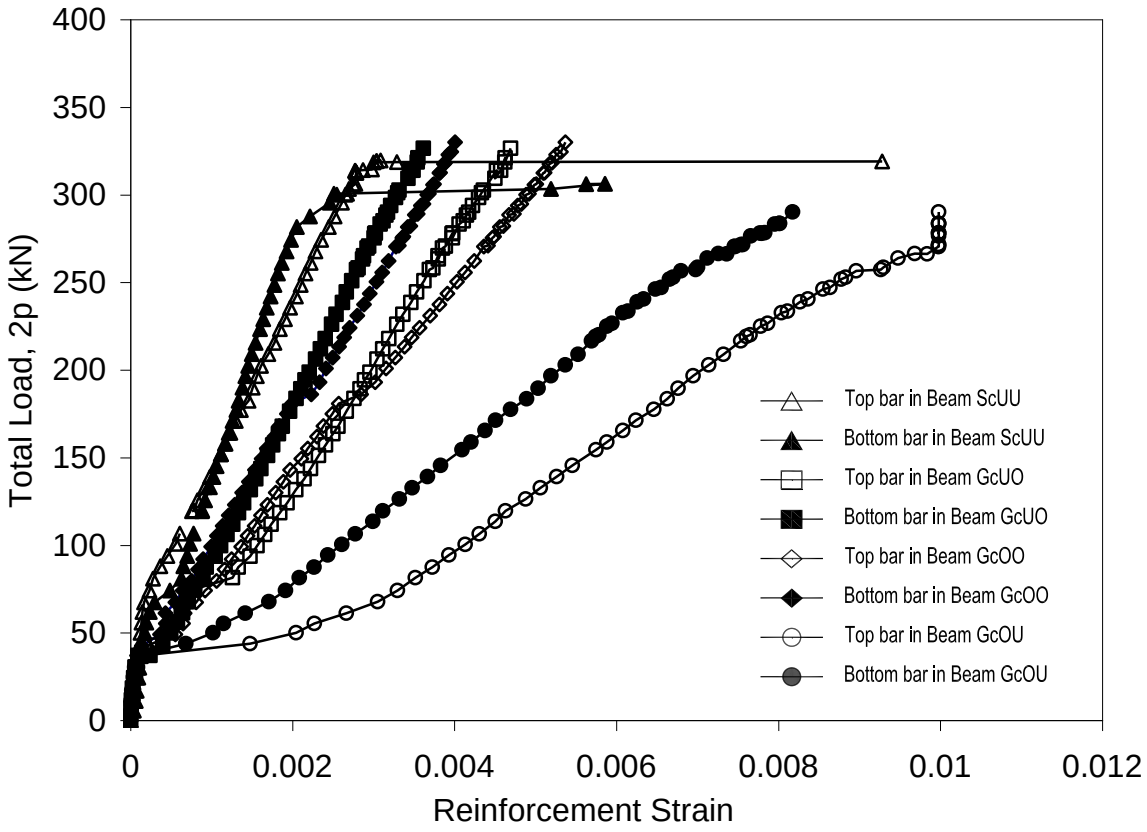


Figure 9: Load –Bar strain relation for continuously supported beams tested

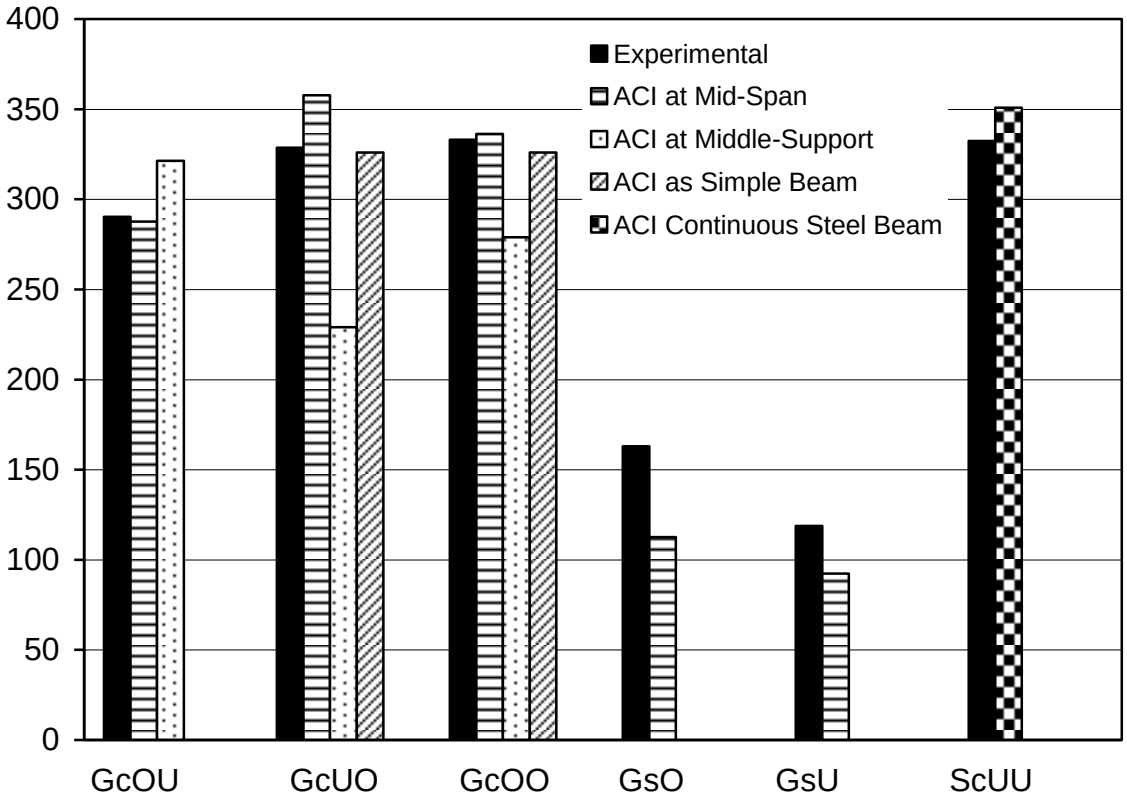


Figure 10: ACI and experimental failure loads

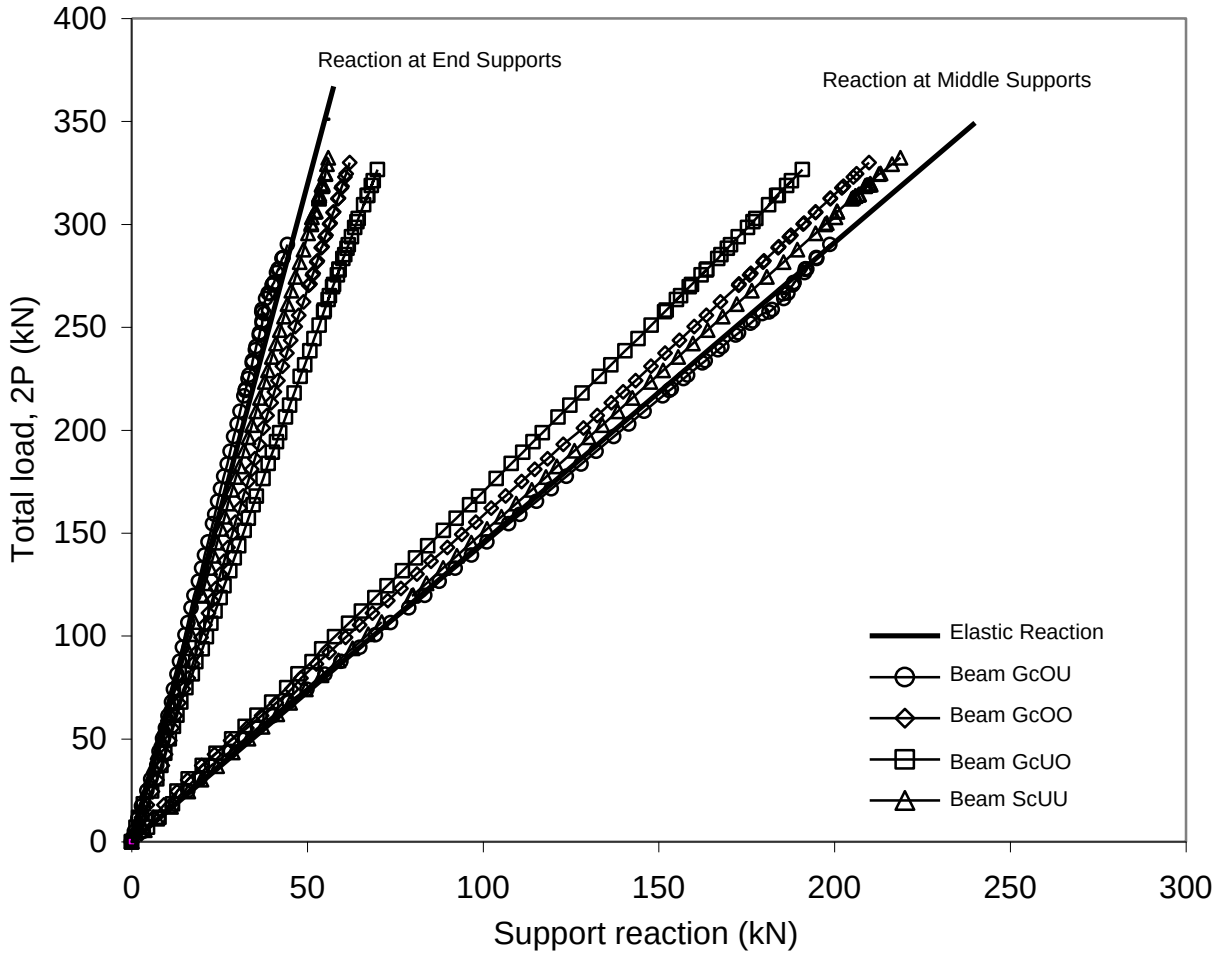


Figure 11: Load-reaction relation for continuously supported beams tested

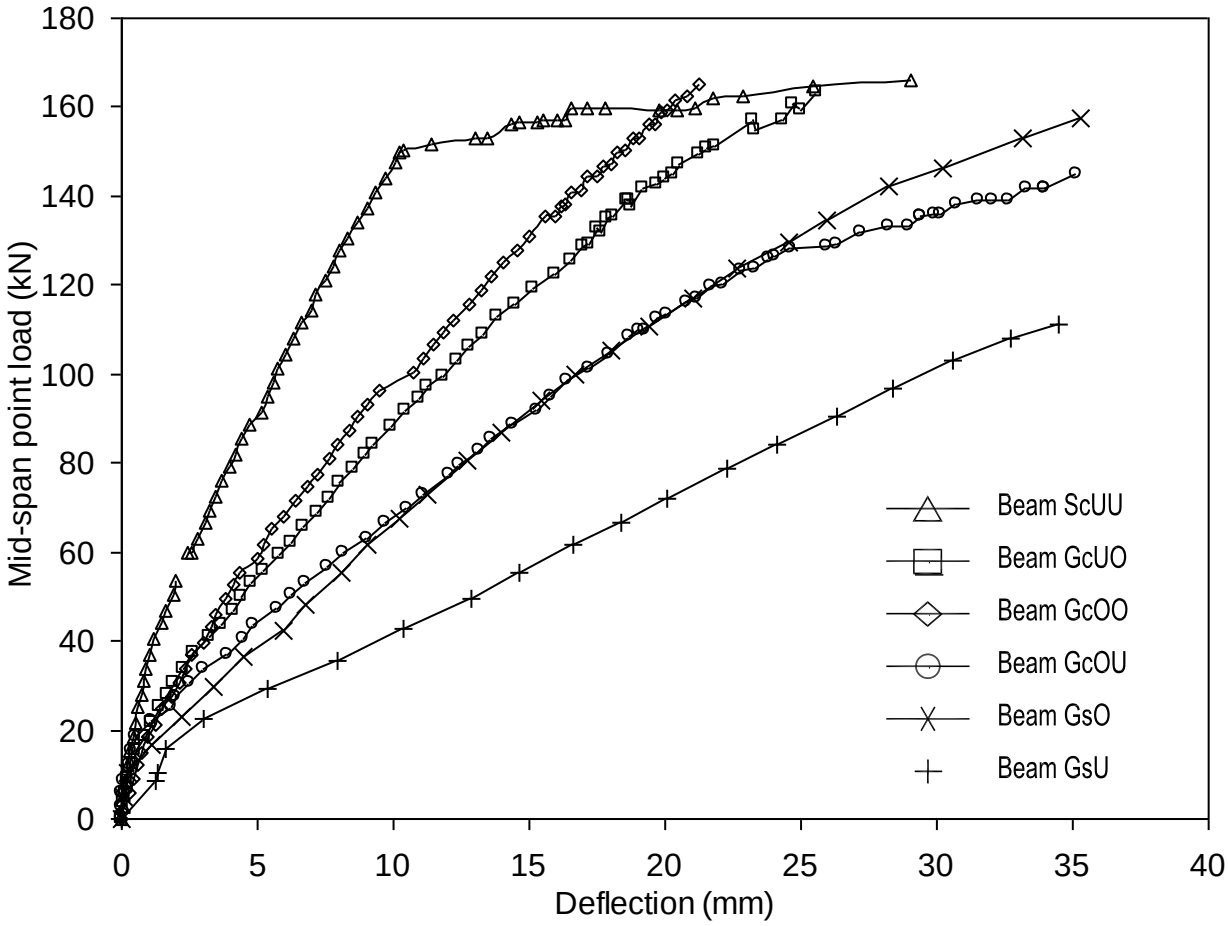


Figure 12: Experimental deflection for beams tested

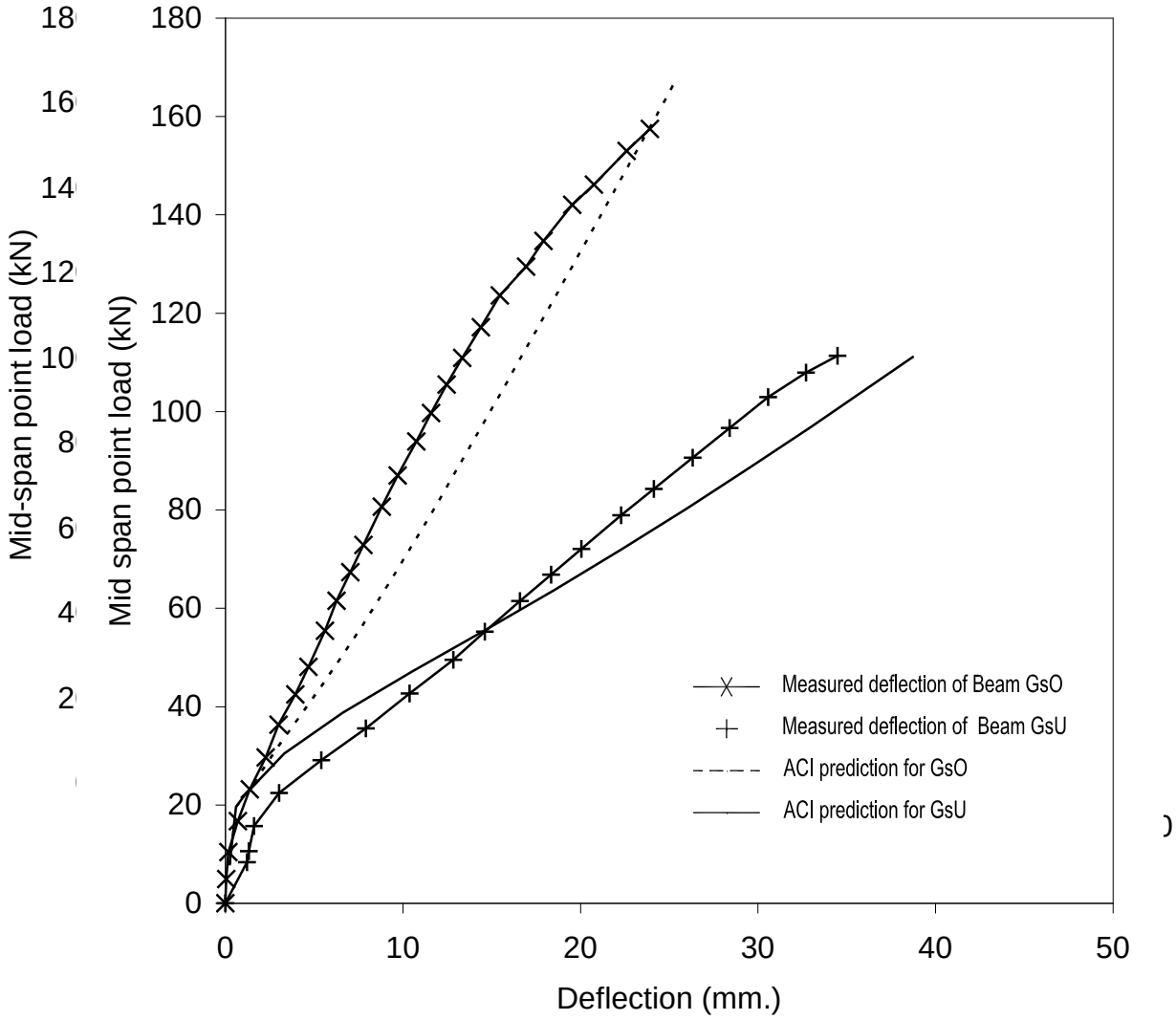


Figure 13: ACI and experimental deflection for simply supported GFRP reinforced beams tested

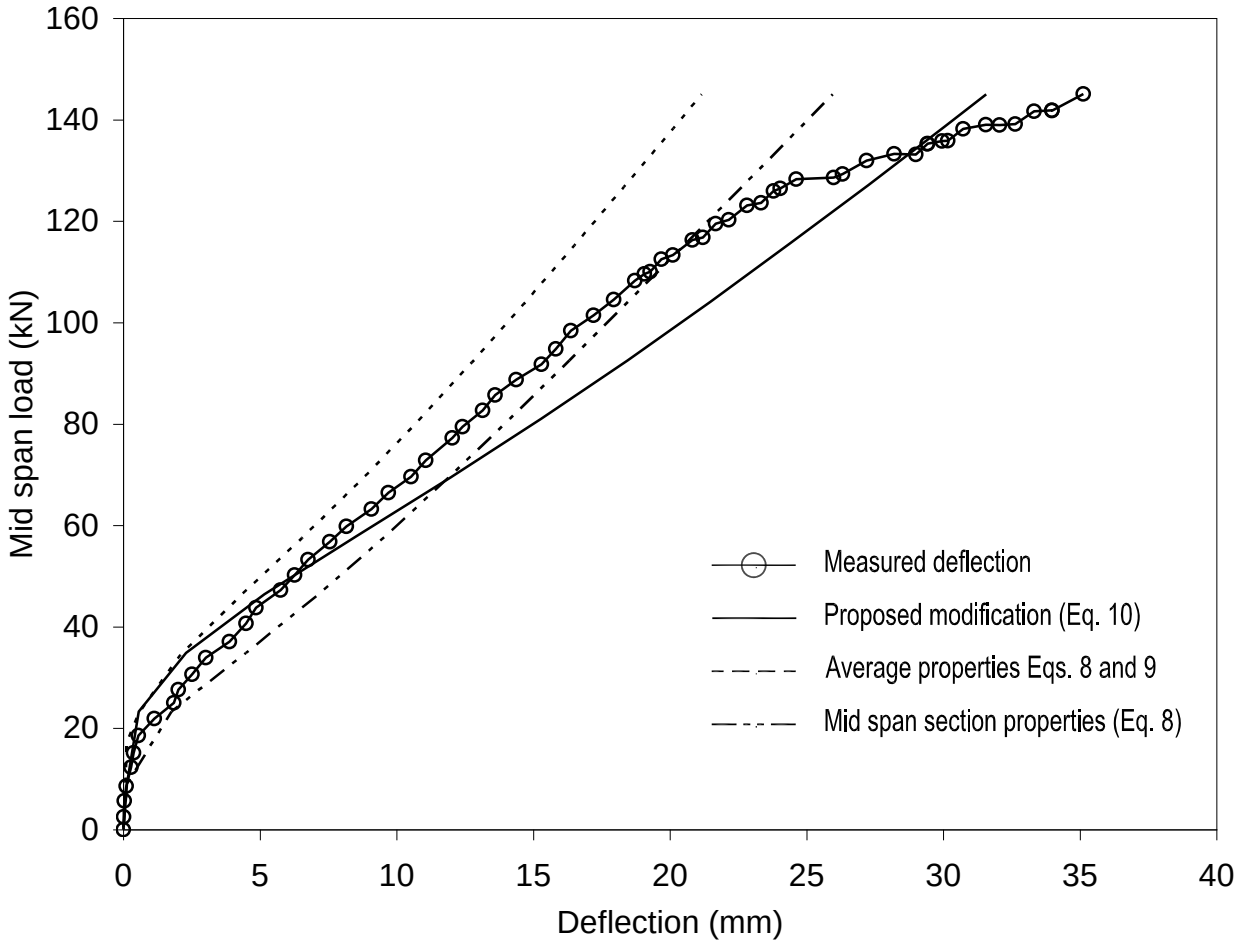


Figure 14: ACI and experimental deflection for beam (GcOU)

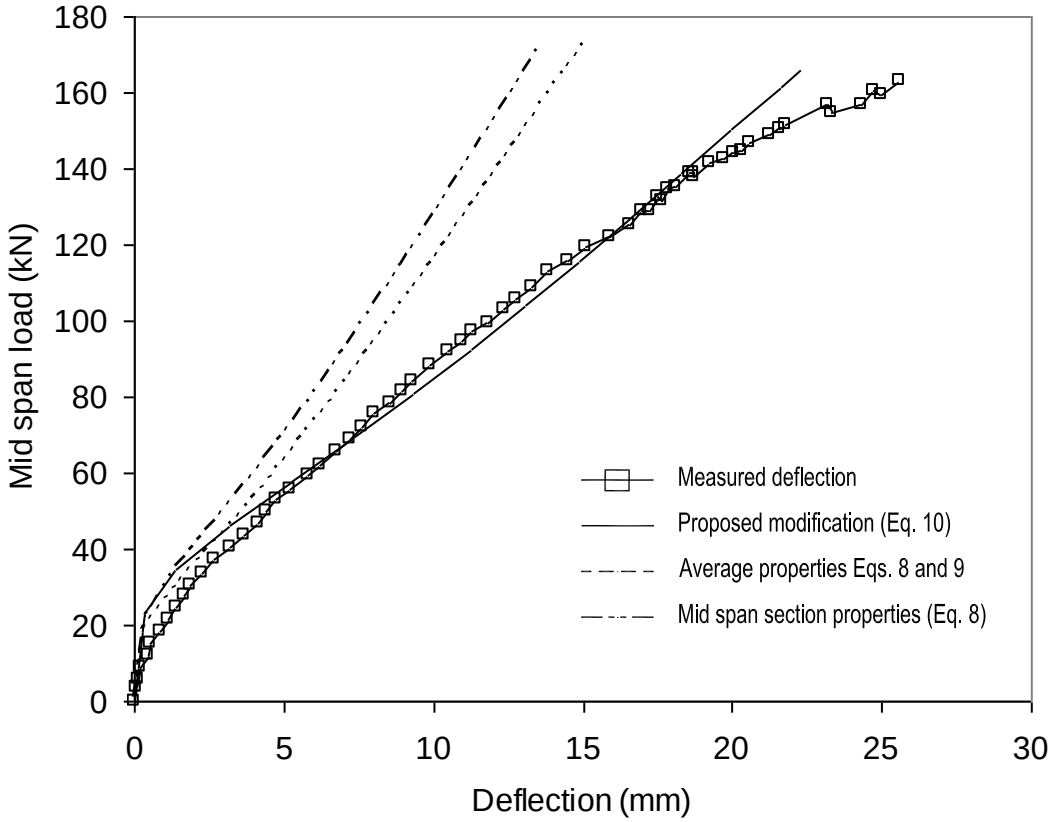


Figure 15: ACI and experimental deflection for beam (GcUO)

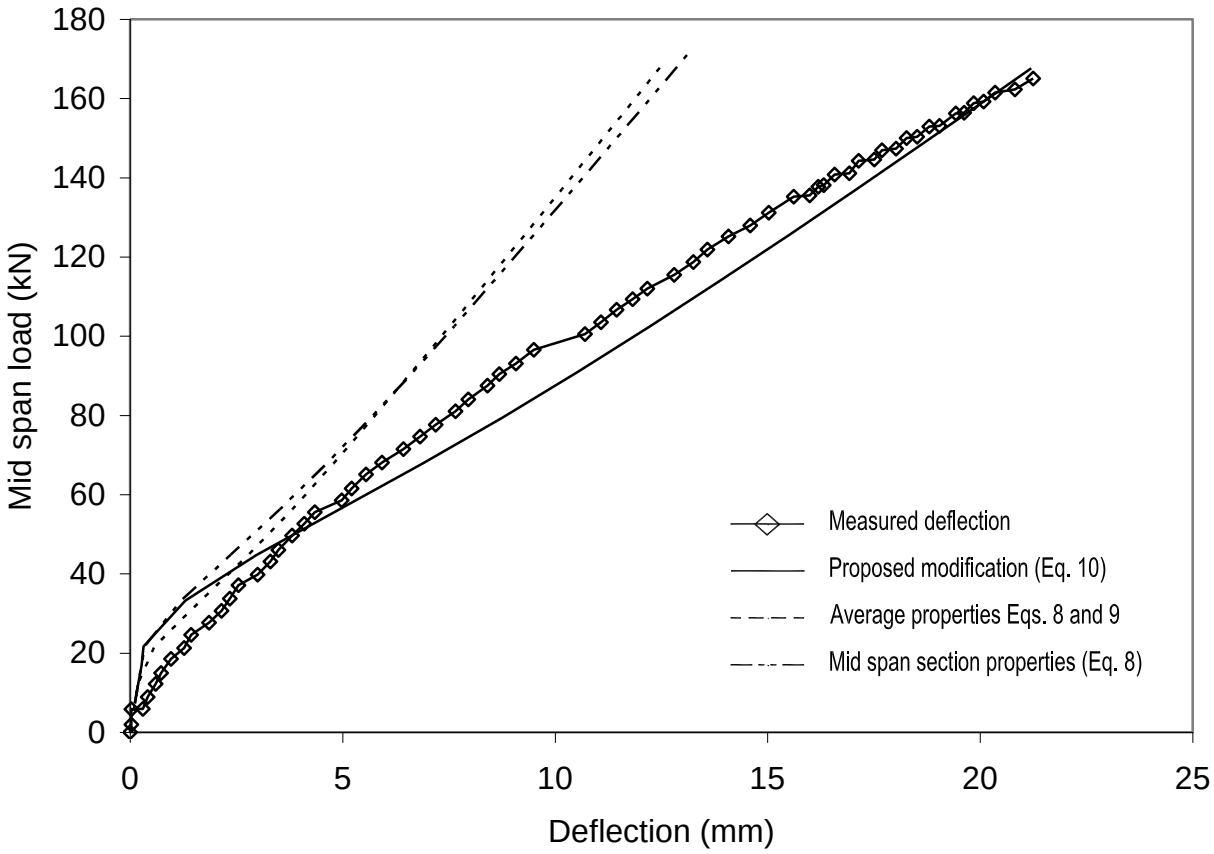


Figure 16: ACI and experimental deflection for beam (GcOO)